



Arsenic(III,V) adsorption onto charred dolomite: Charring optimization and batch studies



Yousef Salameh^a, Ahmad B. Albadarin^{b,c,*}, Stephen Allen^c, Gavin Walker^{b,c}, M.N.M. Ahmad^{a,c}

^a Chemical Engineering, Faculty of Engineering and Architecture, American University of Beirut, Lebanon

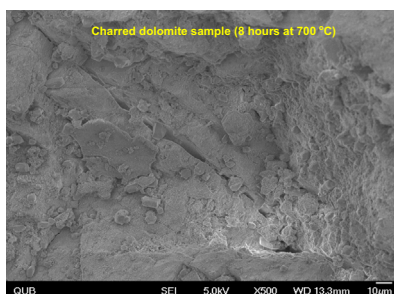
^b Materials Surface Science Institute, Department of Chemical and Environmental Sciences, University of Limerick, Ireland

^c School of Chemistry and Chemical Engineering, Queen's University Belfast, Northern Ireland, UK

HIGHLIGHTS

- The adsorption of arsenic onto thermally processed dolomite was investigated.
- Thermal degradation of the dolomite at 800 °C at 8 h weakens its structure.
- q_{\max} for arsenite and arsenate ions are 1.846 and 2.157 mg/g, respectively.
- Formation of CaCO_3 and MgO accelerated the precipitation of arsenic-carbonate and -oxide.

GRAPHICAL ABSTRACT



ARTICLE INFO

Article history:

Received 29 June 2014

Received in revised form 10 August 2014

Accepted 13 August 2014

Available online 20 August 2014

Keywords:

Arsenite and arsenate
Charred dolomite
Adsorption
Ground-water

ABSTRACT

In this work, the removal of arsenic from aqueous solutions onto thermally processed dolomite is investigated. The dolomite was thermally processed (charred) at temperatures of 600, 700 and 800 °C for 1, 2, 4 and 8 h. Isotherm experiments were carried out on these samples over a wide pH range. A complete arsenic removal was achieved over the pH range studied when using the 800 °C charred dolomite. However, at this temperature, thermal degradation of the dolomite weakens its structure due to the decomposition of the magnesium carbonate, leading to a partial dissolution. For this reason, the dolomitic sorbent chosen for further investigations was the 8 h at 700 °C material. Isotherm studies indicated that the Langmuir model was successful in describing the process to a better extent than the Freundlich model for the As(V) adsorption on the selected charred dolomite. However, for the As(III) adsorption, the Freundlich model was more successful in describing the process. The maximum adsorption capacities of charred dolomite for arsenite and arsenate ions are 1.846 and 2.157 mg/g, respectively. It was found that both the pseudo first- and second-order kinetic models are able to describe the experimental data ($R^2 > 0.980$). The data suggest the charring process allows dissociation of the dolomite to calcium carbonate and magnesium oxide, which accelerates the process of arsenic oxide and arsenic carbonate precipitation.

© 2014 Elsevier B.V. All rights reserved.

1. Introduction

Arsenic contaminated drinking water is a global environmental problem. The chronic toxicity of arsenic in drinking water is known

to cause skin cancer, liver, kidney, and bladder cancers as well as conjunctivitis, melanosis, hyperkeratosis, blackfoot, and in severe cases gangrene in the limbs and malignant neoplasm [1,2]. The area worst affected by this problem is Bangladesh where concentration of arsenic has been reported to be nearly 180 times as high as the WHO limit of 0.01 mg/L for drinking water [3,4]. Increased concentrations of arsenic in natural water have also been reported in many areas all over the world such as China, West Bengal, India,

* Corresponding author at: School of Chemistry and Chemical Engineering, Queen's University Belfast, Northern Ireland, UK.

E-mail address: aalbadarin01@qub.ac.uk (A.B. Albadarin).

Taiwan, Japan, Hungary, Greece, Poland, Serbia, Montenegro, Canada, United States, Argentina, Mexico, Peru and Chile [3,5,6]. Arsenic reaches water supplies as a result of natural conditions such as weathering reactions, biological activity and volcanic emission [7]. Arsenic contamination may also result from anthropogenic activities such as oil and coal burning power plants, electronics industries, dyes and colours, wood preservatives, pesticides, pyrotechnics, drying agents for cotton, oil and solvent recycling [8,9]. Arsenic generally occurs as As(V) and As(III). Arsenate, As(V), is the predominant arsenic form in oxidizing conditions and mainly exists as H_2AsO_4^- and HAsO_4^{2-} while arsenite, As(III), is present mainly as H_3AsO_3 and occurs in reducing environment [10]. Arsenite is considered more toxic than arsenate and tends to be more mobile in the environment [11,12]. Various treatment technologies to remove arsenic from drinking water have been designed such as: coagulation; ion exchange; reverse osmosis; liquid–liquid extraction; and adsorption [13]. However, in many areas of the world there is still a need for appropriate technologies, which are inexpensive, simple to use and easily applied to source use. Consequently, it is important for researchers to design effective technologies for arsenic removal in water and ground-waters. Among various available technologies for decontamination of arsenic, the adsorption method is highly efficient, relatively simple and economical [14,15]. Dolomite, which represents a potential low cost adsorbent, is a common sedimentary rock-forming mineral that can be found in sedimentary beds several hundred feet thick; it is also found in metamorphic marbles, hydrothermal veins and replacement deposits [16–18]. Dolomite is both a mineral and a rock; the dolomite group is composed of minerals with an unusual trigonal bar 3 symmetry. The general formula of this group is $\text{AB}(\text{CO}_3)_2$, where A can be either calcium, barium or strontium and B can be either iron, magnesium, zinc and/or manganese [19]. The amount of calcium and magnesium in most specimens is equal, but occasionally one element may have a slightly greater presence than the other [20]. The majority of dolomite applications use thermal treatment [21–23]. This thermal processing is accompanied by structural changes within the solid product, causing a significant change of the crystallographic, morphological and textural properties [24]. It is obvious, the modification in the interfacial properties of dolomitic solids improves their adsorption properties [25]. The aim of this study was to determine the influence of thermal processing “calcining” on adsorption properties of dolomite for the removal of As(V) and As(III) from aqueous or effluents. The relation between the calcination duration/temperature and the adsorption capacity in terms of impact on the arsenic removal was considered. The effect of experimental parameters including: contact time, solution pH, adsorbent dose along with adsorption isotherms and a possible mechanism were examined.

2. Experimental materials and methods

2.1. Dolomite material

The dolomite was supplied by Kilwaughter Chemical Company, UK. The typical chemical composition of the dolomite in the deposit was 44% MgCO_3 and 53% CaCO_3 [26]. The dolomite was charred at the following temperatures: 600, 700 and 800 °C. Crucibles filled with 40 g dolomite were placed in a furnace which was pre-heated to each of the selected temperatures and left for 1, 2, 4 and 8 h. Thus, in total, 12 samples of charred dolomite were produced. The surface area of raw and charred dolomite was estimated using BET nitrogen adsorption employing a Nova 4200e, surface area and pore size analyser (Quantachrome Instruments). X-ray Diffraction (XRD) analysis was performed to examine the structure of the charred dolomite produced. The equipment employed was a PANalytical X'pert model from Philips. In order

to characterise the adsorption of As(III) and As(V) onto the selected charred dolomite, SEM micrographs of the grain cross-sections were also recorded (JEOL-JSM 6400 scanning microscope). Zeta potentials of raw and charred dolomite were measured as a function of pH using the Zetasizer 3000HS_A with an aqueous capillary flow cell in conjunction with version 1.61 software and the MPT-1 auto titration accessory. Prior to each titration experiment the zeta potential standard DTS0050 was run to ensure the correct functioning of the instrument.

2.2. Stock solutions of arsenite and arsenate

As(V) and As(III) stock solutions were prepared by dissolving accurate amounts of $\text{Na}_2\text{HAsO}_4 \cdot 7\text{H}_2\text{O}$ and NaAsO_2 in deionised water to produce stock solutions of 2000 µg/L. Appropriate dilutions were made to give a range of arsenic concentrations. In addition, 100 mg NaHCO_3 was added to buffer pH fluctuations during the experiment. Most ground-waters have some alkalinity present, which tends to be in the order of 250–600 mg/L NaHCO_3 . The addition of bicarbonate is therefore not seen to compromise the experiment.

2.3. Experimental procedures

Equilibrium experiments were carried out using 0.05 g of the dolomite which was put in contact with 50 mL of arsenic solution ($C_0 = 500$ µg/L). The pH was adjusted to 2, 3, 4, 6, 7, 8, 10 and 11 by using 1 M HCl or 1 M NaOH. The samples were placed in glass jars and subsequently capped and shaken in a mechanical shaker (Gerhardt Bonn type 655) for 5 days at 80 rpm. The same procedures were followed to examine the effect of contact time, adsorbent mass and adsorption isotherms. The C_0 values of As(III) and As(V) for the contact time studies were 50, 500, 1000 and 2000 µg/L. Again, to study the effect of mass-volume ratio, the amounts of charred dolomite were varied and mixed with solution of As(III) and As(V) with C_0 values as above. To obtain adsorption equilibrium isotherms, the effect of initial arsenic concentration was undertaken at room temperature by varying the initial concentration 50–2000 µg/L. A mass of 0.05 g of charred dolomite was mixed with 50 mL of arsenic solution and the mixture was continuously shaken for 5 days. After equilibrium, samples were filtered through a 0.45 µm cellulose nitrate membrane filter (Swinnex-25 Millipore) and prepared for analyses using ICP-AES. The samples were made up to 10 ml to give a 2% nitric acid solution. All experiments were conducted at the room temperature (20 °C). Each experiment was repeated and mean values were used. There were no pH adjustments for contact time, adsorbent dose and isotherm experiments. Percentage solute removal and amount adsorbed per unit mass of adsorbent q in (mg/g) was then calculated as follows:

$$\text{Percentage removal} = \left[1 - \frac{C_e}{C_0} \right] \times 100\% \quad (1)$$

$$q = \left[\frac{C_0 - C_e}{M} \right] \times V \quad (2)$$

where C_0 and C_e (mg/L) are the initial and equilibrium solute concentrations, respectively.

3. Results and discussion

3.1. Dolomite charring optimisation and characterisation

3.1.1. Charring optimisation

The thermal decomposition of dolomite occurs in air in two steps, as follows [27,28]:

First reaction : $\text{CaMg}(\text{CO}_3)_2 \rightarrow \text{CaCO}_3 + \text{MgO} + \text{CO}_2$

Second reaction : $\text{CaCO}_3 \rightarrow \text{CaO} + \text{CO}_2$

When decomposition of dolomite is stopped after the first step, the product is a solid consisting of a rigid, porous calcite and the fine powdered magnesium oxide [29]. According to Stefaniak and co-worker [27], the thermal decomposition process can be controlled precisely only at a temperature of 800 °C, because of the two-step reaction of dissociation. Generally, the product of partial decomposition of dolomite contains calcium carbonate (calcite) and magnesium oxide and shows a significant increase in specific surface area and pore volume [30]. The formation of CaCO_3 and MgO after charring allows the formation of arsenic oxide and arsenic carbonate, so precipitation of these compounds will take place and thus the arsenic removal will increase.

3.1.2. Dolomitic adsorbent characterisation

The surface area of the raw dolomite was found to be 0.89 m²/g. Table 1 shows that the charring procedure has a significant effect on the cumulative surface area. A clear correlation between the surface areas and the charring duration and temperature can be observed; the surface area increases with an increase in the charring duration and temperature. The increase in the surface area of the charred dolomite will facilitate the adsorption of the arsenic ions onto the charred dolomite. The XRD for the 8 h at 700 and 800 °C charred dolomite is given in Fig. 1. It was found that both charred dolomites i.e. charred at 700 and 800 °C mainly comprised of CaO , MgO , $\text{Ca}(\text{OH})_2$ and $\text{CaMg}(\text{CO}_3)_2$. The XRD data shows a trace of magnesium oxide, which is a proof that charring the dolomite at 700 °C for 8 h is sufficient to cause the dissociation of some magnesium carbonate to magnesium oxide. There was also a small presence of calcium hydroxide, which is a result of the grinding procedure when partial decomposition of dolomite have occurred. It may be the case that while the temperature is not sufficient to

cause the thermal dissociation of CaCO_3 in the bulk particles, it may be sufficient to cause the partial dissociation of the fine dolomite particles resulted from grinding on the surface of the dolomite. The absence of magnesium hydroxide was also noted. This indicates that the MgO formed is insufficiently reactive to form magnesium hydroxide with the water vapour present in the air. The SEM images in Fig. 2A and 2B show the surface of charred dolomite (8 h at 700 °C); the surface looks “muddy” with the presence of some sharp edges. The presence of fine particles at the surface of the samples underlines the very brittle nature of the materials used in the study. The formation of new crystals on the surface of the charred dolomite, in Fig. 2C, implies a precipitation-adsorption process for arsenic removal. Fig. 2C also illustrates the formation of new pores and voids alongside the formation of new crystals on the surface of the selected dolomite. This suggests that the adsorption of As(III) may have been facilitated by meso- and macro-pore development. The less obvious surface structure change after As(V) adsorption onto charred dolomite in Fig. 2D indicates that surface precipitation is not the main removal mechanism. Finally, the zero charge point (PZC) of charred dolomite (8 h at 700 °C) was determined as 10; below this value, the surface of dolomite and charred dolomite is positively charged.

3.2. Effect of pH

The effect of pH on the As(III) and As(V) removal from aqueous solution using charred dolomite is illustrated in Figs. 3 and 4 ($C_0 = 500 \mu\text{g/L}$). The figures show that As(III) and As(V) were completely removed by the dolomite samples which have been charred to 800 °C at different charring times over the pH range studied. Usually, the adsorption of arsenic species is highly dependent on pH because As(III) exists in solution as H_3AsO_3 at pH 0–9 and as H_2AsO_3^- in the pH 10–12, whereas As(V) exists as H_3AsO_4 at pH 0–2, H_2AsO_4^- at pH 3–6 and HAsO_4^{2-} at pH 7–11 [31]. In this study, the solution pH did not seem to have any obvious impact on the adsorption capacity of either the arsenite or the arsenate when the dolomite was charred at 600, 700 and 800 °C. However, it can be observed that As(V) was adsorbed in larger quantities than As(III). Similar observations were reported for the adsorption of arsenic onto zirconium- and titanium-modified sorbents [32]. This wide-ranging optimum pH is explained by the amphoteric nature of charred dolomite, as MgO and CaCO_3 minerals chiefly attributed to As(III) and As(V) removal. It is worth mentioning that from the zeta potential values of the charred dolomite, no isoelectric points were recorded and the charred dolomite material exhibited a positive potential over all the pH range studied (data not shown). This

Table 1
Surface areas of charred dolomite.

Charring duration (h)	Charring temperature		
	600 °C	700 °C	800 °C
	Surface area (m ² /g)		
1	1.32	2.83	5.6
2	2.45	3.41	6.15
4	3.58	5.73	10.86
8	3.95	7.31	11.81

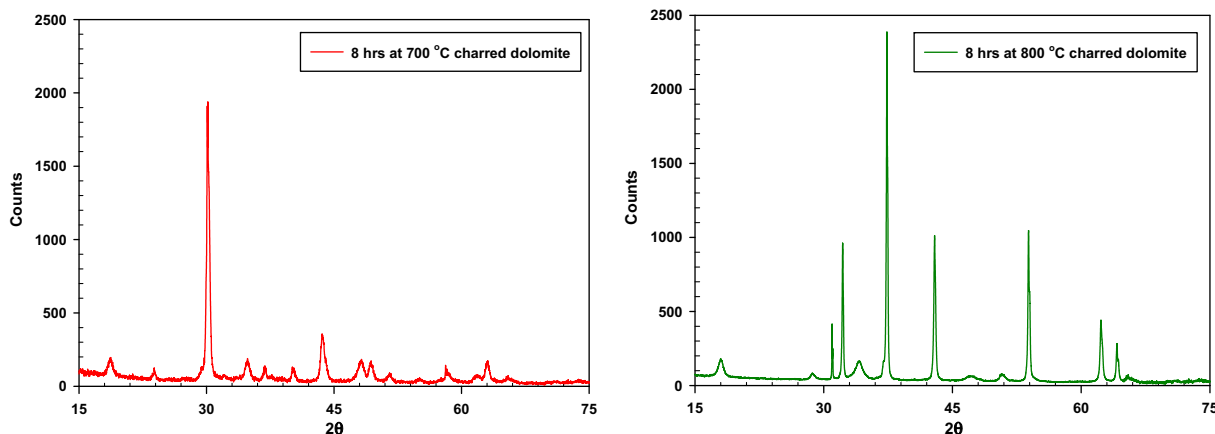


Fig. 1. XRD profiles for 8 h at 700 and 800 °C charred dolomite.

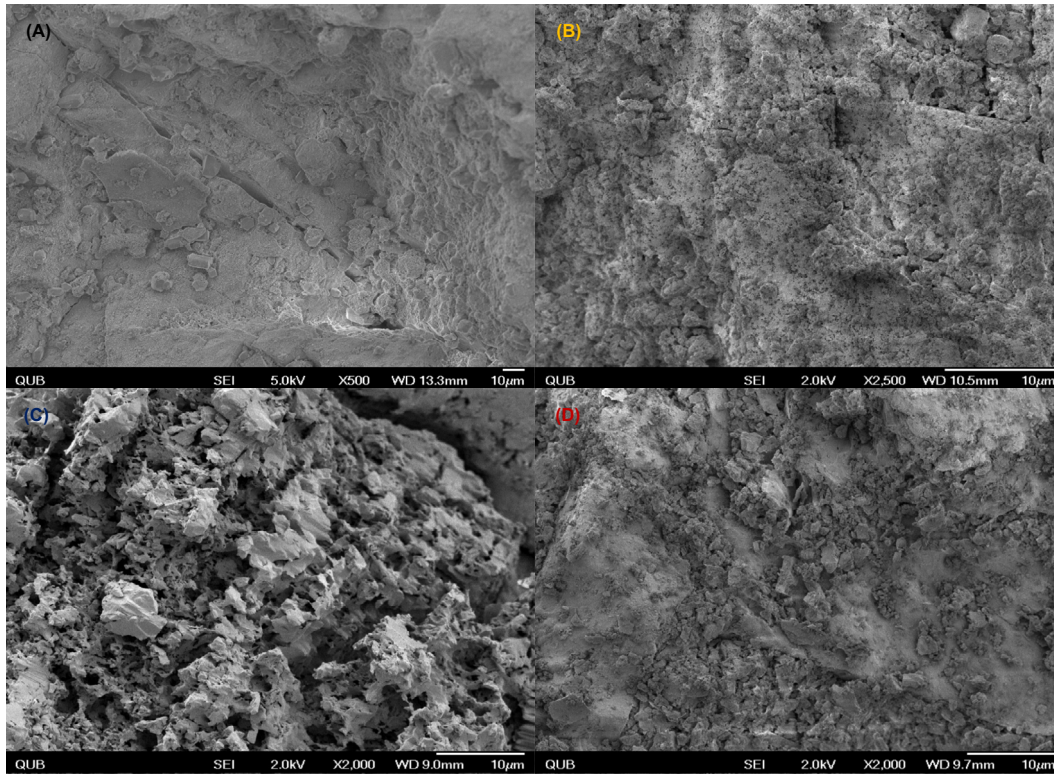


Fig. 2. SEM of surface of charred dolomite (8 h at 700 °C) sample ((A) and (B)) after the adsorption of As(III) (C) and As(V) (D).

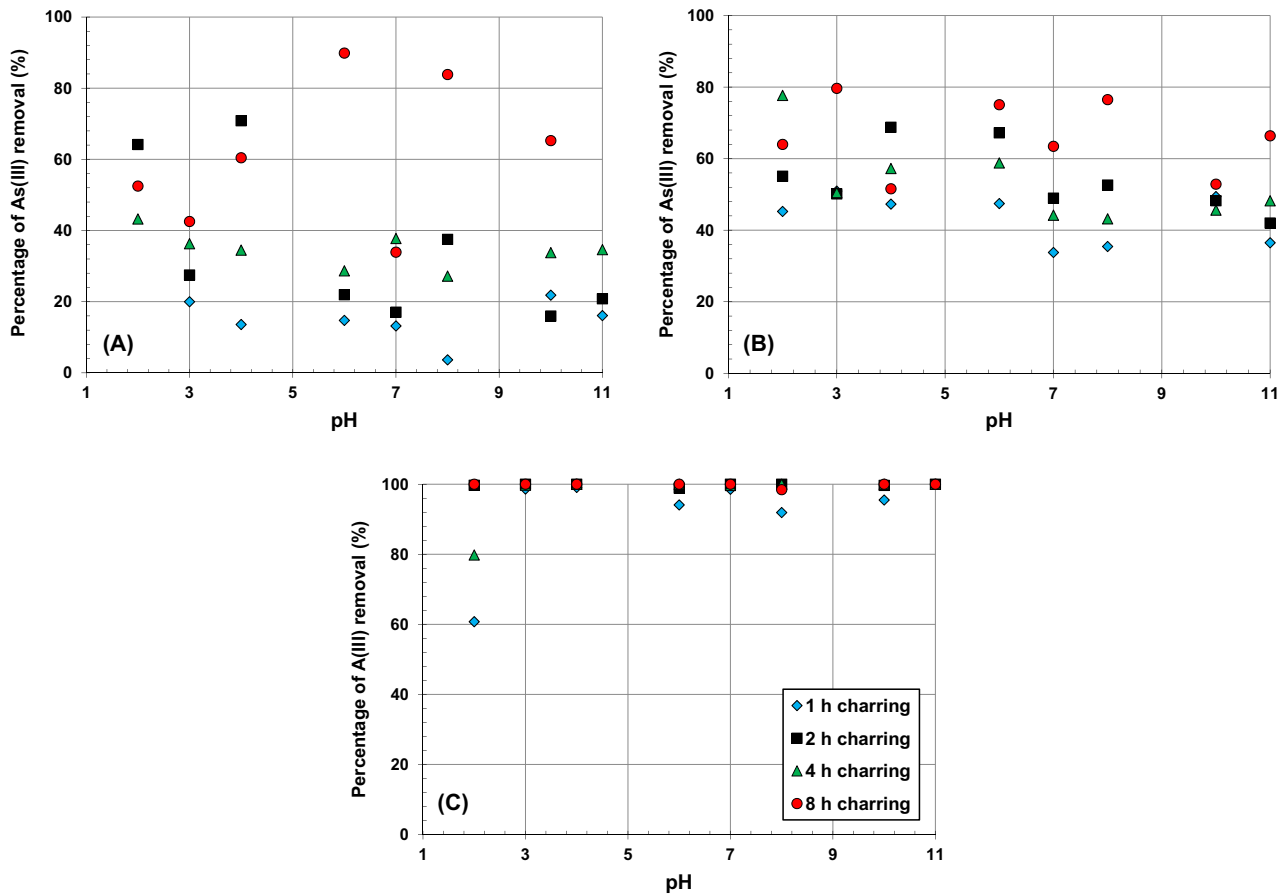


Fig. 3. The pH dependence of As(III) adsorption onto (A) 600 °C, (B) 700 °C and (C) 800 °C charred dolomite for different charring times. Adsorbent dose: 1 g/L; $C_0 = 500 \mu\text{g/L}$; contact time: 5 days at 20 °C.

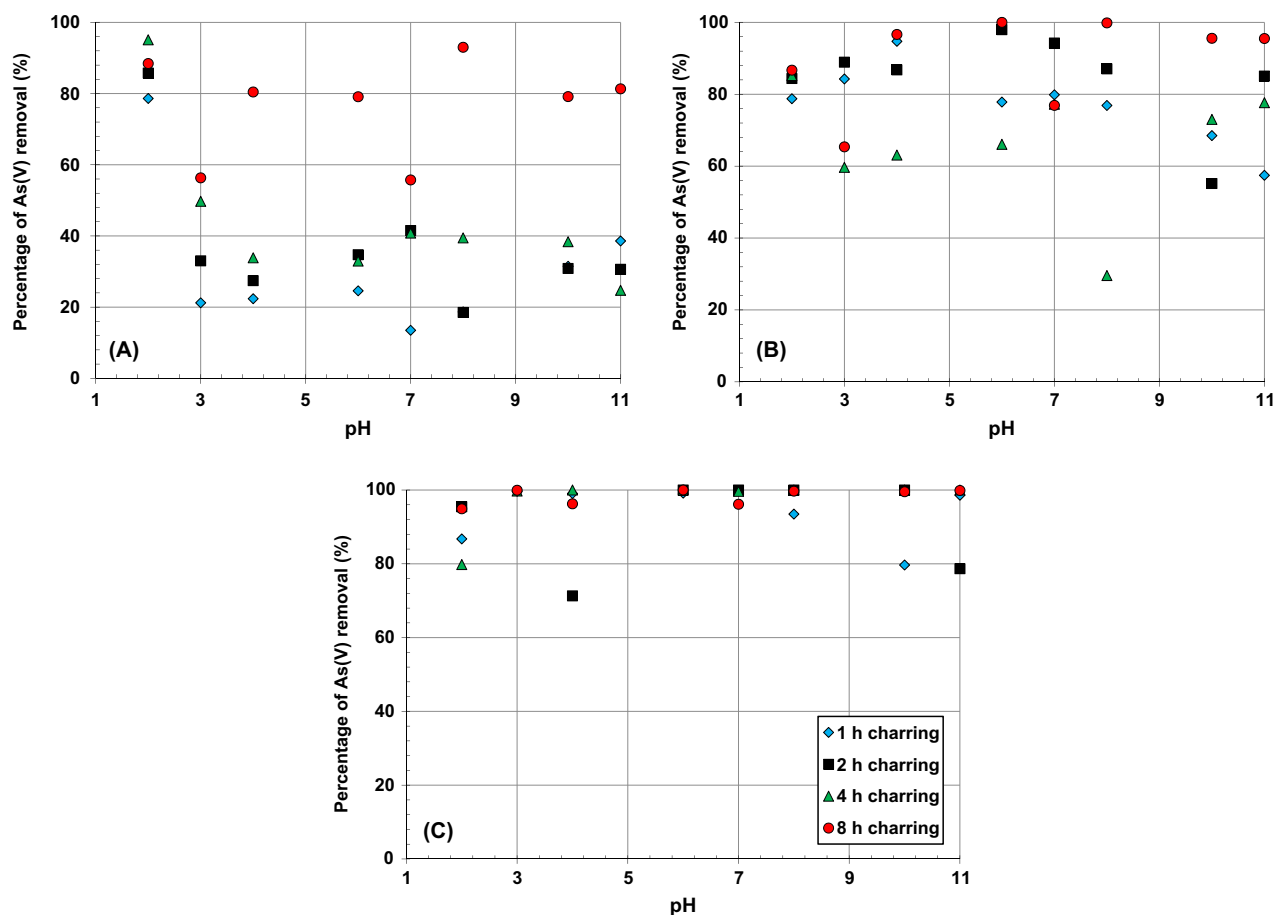


Fig. 4. The pH dependence of As(V) adsorption onto (A) 600 °C, (B) 700 °C and (C) 800 °C charred dolomite for different charring times. Adsorbent dose: 1 g/L; $C_0 = 500 \mu\text{g/L}$; contact time: 5 days at 20 °C.

may explain the successful removal of arsenic species by this charred dolomite over the pH range studied.

However, the dolomite that has been charred for 8 h at 800 °C was found to dissolve in the solution during the adsorption process. This can be attributed to the fact that during the thermal processing, or “calcining” process, the magnesium carbonate components of the dolomite decompose at temperatures around 800 °C [33]. The dolomite charred for 8 h at 700 °C was almost as good as the dolomite which was charred at 800 °C in removing both As(III) and As(VI). For that reason, the later studies were conducted using the 8 h at 700 °C charred dolomite.

3.3. Effect of adsorbent mass

Adsorption process occurs when an interaction (chemical or physical) takes a place between the adsorbate and the adsorbent. So it is expected that the relationship between the dolomite mass (at fixed particle size or diameter) and the amount of the arsenic adsorbed is proportional i.e., more arsenic would be adsorbed in the presence of higher dolomite mass [34]. The increase in the efficiency of removal can be attributed to increased adsorbent surface area available for mass transfer i.e., more pores and voids for the arsenic chemisorption, also higher concentrations of MgCO_3 and CaCO_3 which would increase the probability of the formation of arsenic oxide and arsenic carbonate, thus increasing the extent of precipitation as a mechanism of arsenic removal. The effect of adsorbent mass to volume of solution on arsenic uptake is illustrated in Fig. 5, which shows that the adsorption efficiency of arsenic increased with an increase in mass of charred dolomite. It can be noted from Fig. 5 that the plateau (which represents the

maximum adsorption capacity of the adsorbent when the surface is saturated with the adsorbate molecules) can only be drawn in the case of lowest concentration of charred dolomite (0.5 g). When higher concentrations of charred dolomite are used, with the same concentrations of arsenic, no plateau can be drawn, higher concentrations of arsenic may be used to attain the plateau. This is evidence of the dolomite high capacity and affinity to arsenic. Higher mass provides a larger area and a larger number of adsorption sites, which help to lower the competition between the arsenic ions for active sites and accelerate the adsorption reaction. The dosage chosen for kinetic and batch experiment, however, does not necessarily have to be the optimum dosage. In our study, the adsorbent concentration was set at 1 g/L in the batch experiments.

3.4. Effect of contact time

The plots of q_t versus t at different initial As(III) and As(V) concentrations are shown in Fig. 6. Inspection of the curves shows that the kinetics adsorption curves are smooth and continuous leading to saturation of charred dolomite by arsenic. This suggests the possibility of monolayer coverage adsorption of arsenic onto charred dolomite [35]. The adsorption rates were rather fast at low initial concentrations of arsenite and arsenate. In contrast, it can be seen that the adsorption is relatively slow at initial concentrations equal to or higher than $500 \mu\text{g/L}$. See Fig. 6 (the fractional uptake f against time t plots; where $f = q/q_e$) for a more obvious indication concerning how close the adsorption system at time t is towards its equilibrium state [16]. The adsorption was fast in the initial stage caused by the large number of available sites, resulting in a

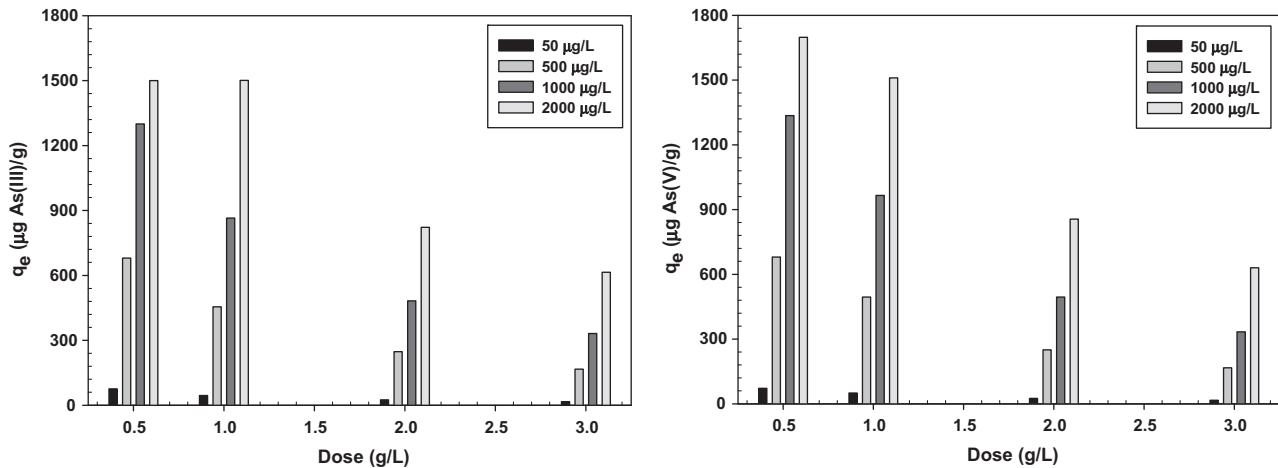


Fig. 5. Effect of adsorbent dose for the adsorption of As(III) and As(V) from aqueous solution onto charred dolomite (8 h at 700 °C). Adsorbent dose: 1 g/L; contact time: 5 days at 20 °C.

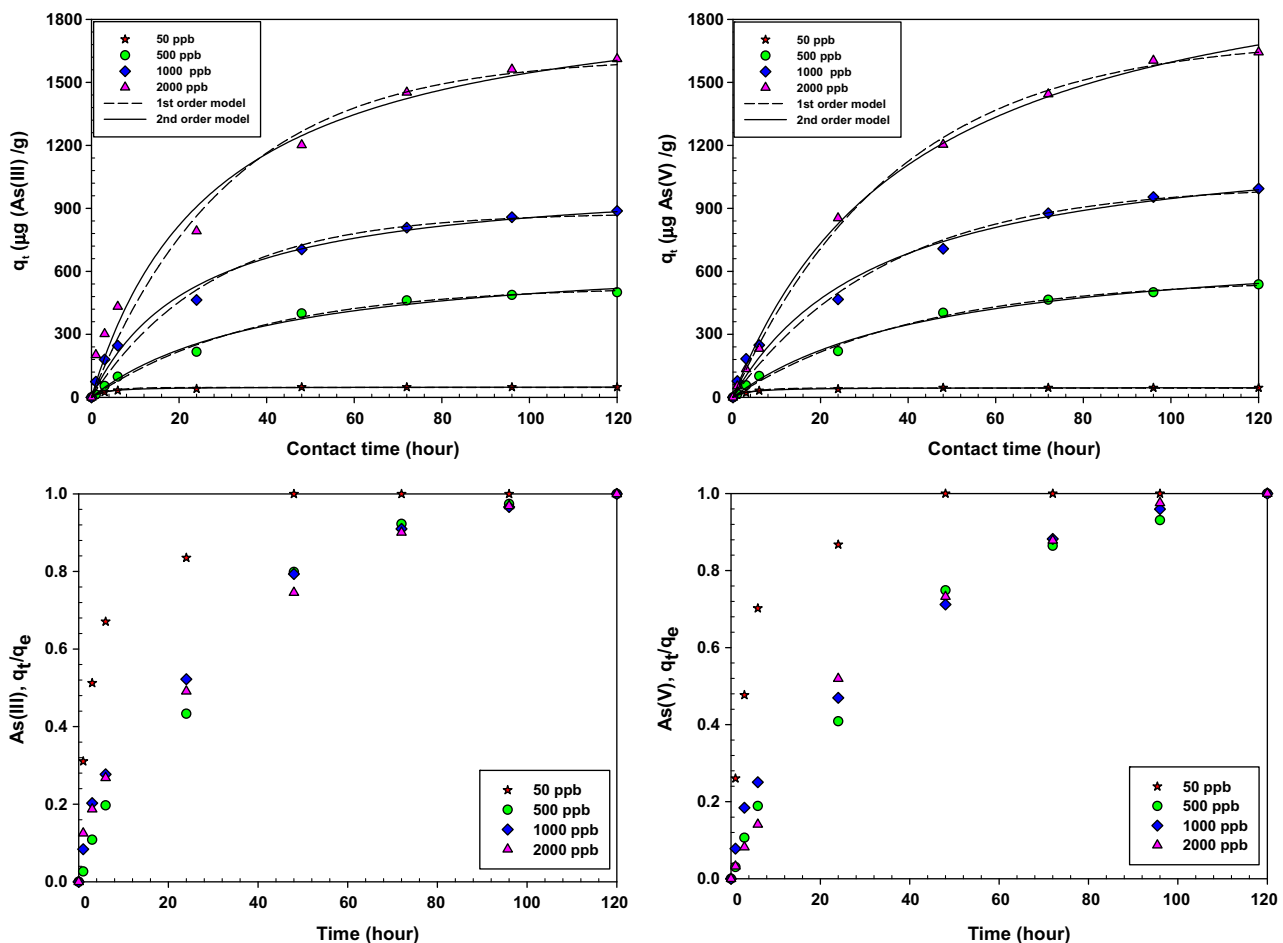


Fig. 6. Kinetics of As(III) and As(V) adsorption by the charred dolomite (8 h at 700 °C) at the fitting of pseudo first-order and second-order models different initial concentrations and fractional approach to equilibrium with time.

concentration gradient. The removal rate gradually declined with time due to an increase in surface coverage until equilibrium was attained [17]. The equilibrium time of 48 and 24 h was required for solutions of 50 µg/L initial concentrations of As(III) and As(V), respectively. On the other hand, for higher initial concentrations of 500, 1000 and 2000 50 µg/L, longer time was needed for the system to reach equilibrium. After this, the increase in contact time might not help for more sorption of metal ions with this sorbent.

3.5. Kinetic modelling

The pseudo first- [36] and pseudo second-order [37] models (Eqs. (3) and (4)) have been employed to examine the contact time data for the adsorption of As(III) and As(V) by non-linear regression. The pseudo first-order model equation is given as follows:

$$q_t = q_e(1 - e^{-k_1 t}) \quad (3)$$

Table 2

Kinetic parameters and correlation coefficients for As(III) and As(V) adsorption onto charred dolomite (8 h at 700 °C).

	C_0 (ppb)	Pseudo first-order model				Pseudo second-order model			
		$q_{e,exp}$ (mg/g)	$q_{e,cal}$ (mg/g)	k_1 (1/h)	R^2	$q_{e,cal}$ (mg/g)	$k_2 \times 10^{-5}$ (g/mg h)	h	R^2
As(III)	50	0.048	0.046	0.242	0.965	0.049	0.007*	1.68×10^{-5}	0.990
	500	0.500	0.529	0.027	0.991	0.699	3.421	1.671	0.992
	1000	0.888	0.879	0.036	0.981	1.061	3.916	4.408	0.990
	2000	1.612	1.620	0.031	0.980	1.986	1.765	6.961	0.988
As(V)	50	0.045	0.044	0.227	0.984	0.046	0.007*	1.48×10^{-5}	0.996
	500	0.537	0.564	0.024	0.992	0.757	2.778	1.591	0.994
	1000	0.993	1.012	0.028	0.980	1.269	2.305	3.711	0.988
	2000	1.644	1.713	0.027	0.999	2.262	1.059	5.418	0.998

* No power required.

The pseudo second-order equation is given as:

$$q_t = \frac{k_2 q_e^2}{(1 + k_2 q_e t)} t \quad (4)$$

The initial sorption rate given by [34]:

$$h = k_2 q_e^2 \quad (5)$$

where k_1 (1/min) and k_2 (g/mg min) are the rate constants for first-order and second-order models.

The plots of pseudo first- and second-order models at different arsenic concentration are shown in Fig. 6 and values of the constants of kinetic models found from the plots are given in Table 2. It can be seen that both the pseudo first- and second-order kinetic models are able to describe the experimental data ($R^2 > 0.980$). The values of R^2 show the ability of the pseudo second-order model to represent the experimental results to a higher degree of accuracy ($R^2 > 0.988$). Though, from Table 2, the q values ($q_{e,cal}$) determined from pseudo first-order model were closer to the experimental q values ($q_{e,exp}$) than those determined from the pseudo second-order model. It is worth noting that the pseudo kinetic models should be treated as empirical equations that do not offer an exact representation of the chemical and physical processes [38]. It was found that the initial rate of adsorption (h) increases with an increase in the initial As concentration. The non-linear relations between the rate constants and the initial As concentration in Table 2 indicates that mechanisms such as ion exchange and physical adsorption are involved in the adsorption process [39]. However, a larger k_1 value suggests that adsorption systems with low concentrations will require a shorter time to reach a specific fractional uptake [15].

3.6. Isotherm modelling

To determine the adsorption capacity for arsenic on charred dolomite (8 h at 700 °C) and for process design purposes, equilibrium adsorption isotherm data are of fundamental importance [40]. Three of the most commonly used isotherm models, Langmuir, Freundlich and Redlich–Peterson models, were applied. The form of the Langmuir equation can be represented as follows [41]:

$$q_e = \frac{q_{max} b C_e}{1 + b C_e} \quad (6)$$

where q_e is the solid phase solute concentration (mg/g); q_{max} is the maximum arsenic uptake capacity (mg/g) and b is the equilibrium constant (L/mg).

The Freundlich model has the following form [42]:

$$q_e = K_F C_e^{1/n} \quad (7)$$

where K_F is the constant indicative of the relative adsorption capacity of the adsorbent (mg/g)(L/mg) $^{1/n}$ and $1/n$ is the constant indicative of the intensity of the adsorption and is dimensionless.

The Redlich–Peterson model is given below [43]:

$$q_e = \frac{K_R C_e}{1 + a_R C_e^\beta} \quad (8)$$

where K_R (L/g) and β are the Redlich–Peterson isotherm constant (L/mg $^{1-1/K_R}$) and a_R is the exponent, which lies between 0 and 1.

The Langmuir, Freundlich and Redlich–Peterson isotherm plots for As(III) and As(V)-8 h at 700 °C charred dolomite systems are shown in Fig. 7. The shapes of adsorption curves for both As(III) and As(V) are similar i.e. the adsorbed amount increased with

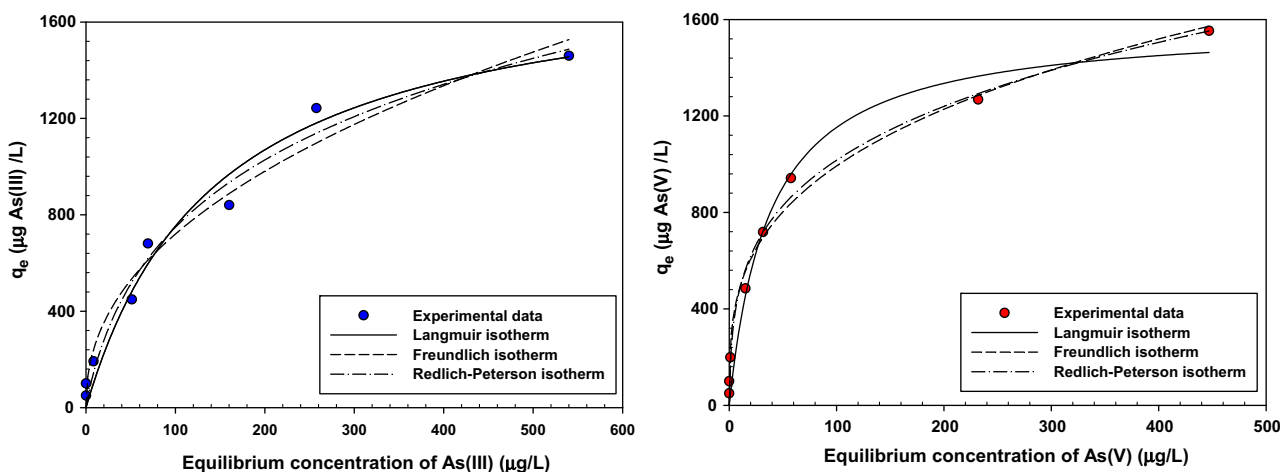


Fig. 7. Isotherm plots for the adsorption of As(III) and As(V) onto charred dolomite (8 h 700 °C).

Table 3
The Langmuir, Freundlich and Redlich–Peterson parameters and correlation coefficients for As(III) and As(V) adsorption onto charred dolomite (8 h at 700 °C).

	Langmuir isotherm model			Freundlich isotherm model			Redlich–Peterson model			
	q_{\max}	b	R^2	K_F	n	R^2	K_R	a_R	β	R^2
As(III)	1.846	0.007	0.972	92.41	2.243	0.978	21.64	0.056	0.764	0.976
As(V)	2.157	0.026	0.985	260.1	3.254	0.975	34.58	1.143	0.730	0.982

Where: q_{\max} : (mg/g); b : (L/mg); K_F : (mg/g)(L/mg)^{1/n} and K_R : (L/g).

Table 4
Comparison of adsorption capacities of the charred dolomite with other adsorbents in literature (After [44]).

Adsorbent	pH	Surface area (m ² /g)	Concentration	Adsorption capacity (mg/g)	
				As(III)	As(V)
Charred dolomite	7.2	13.67	50–2000 µg/L	1.846	2.157 This study
Char carbon	2–3	36.48	157–737 µg/L for As(V) and 193–992 µg/L for As(III)	89.00	34.46
Red mud (RRM)	7.25 for As(III); 3.50 for As(V)	–	33.37–400.4 µmol/L	0.663	0.514
Gibbsite	5.5	13.50	10–1000 mg/L	3.300	4.600
GAC	7.0	1.065	1 mg/L	0.090	4.500
Polymetallic sea nodule	6.0 for As(III); 2.0 for As(V)	–	0–0.7 mg/L for As(III); 0–1.0 mg/L for As(V)	0.690	2.85

increasing concentration. Adsorption isotherm parameters and correlation coefficients for As(III) and As(V) adsorption onto charred dolomite are given in Table 3. It can be observed that all Langmuir and Freundlich parameters of As(V) adsorption are higher than that of As(III) adsorption, which is attributable to the predominant species of arsenic being; As(III) i.e. H₃AsO₃ (pK_{a1} = 9.2) and whereas for As(V) H₂AsO₄[−] (pK_{a1} = 6.7) present at neutral pH. Based on regression coefficient (R^2) values, the adsorption of As(III) has been well described by the Freundlich model. It follows therefore that the adsorption is not limited to a monolayer, and that As(III) molecules migrate to heterogeneous surfaces on the charred dolomite following the Freundlich isotherm theory. While, Langmuir model represented the As(V) adsorption adequately. The R_L values for the range of the arsenic concentrations under investigation have been calculated and found to lie between 0 and 1, which indicated that the sorption of As(III) and As(V) by the charred dolomite is favourable at the neutral pH and temperature 20 °C. The Redlich–Peterson isotherm is also revealed in Fig. 7. Generally, the values of the correlation coefficient (R^2) indicated that the Redlich–Peterson isotherm can also be used to describe to the experimental data.

3.7. Comparison of adsorption capacity with composite adsorbents

A comparison was performed between the results of the adsorption capacities of charred dolomite and other adsorbents towards arsenite and arsenate (Table 4); the different experimental conditions used were not taken into account. The comparison showed that charred dolomite can be considered as one of the most effective adsorption systems for this purpose. This is evidence of the dolomite high capacity and affinity to arsenic. It should be noted that dolomite is an inexpensive material compared to commercial adsorbents e.g., activated carbon, therefore increasing the dolomite mass in order to accelerate the arsenic sorption may still be a cost effective method for treatment [44].

4. Conclusions

The maximum removal of arsenite and arsenate was found with the dolomite samples which were charred to 800 °C at 8 h, but thermal degradation of the dolomite at this temperature, leads to the partial dissolution of this charred dolomite on contact with water. The optimum dolomitic sorbent chosen for further investigations was the 8 h at 700 °C material. Initial investigations on this

charred dolomite have been undertaken to determine its potential as an adsorbent. The data suggest the charring process allows dissociation of the dolomite to calcium carbonate and magnesium oxide, which accelerates the process of arsenic oxide and arsenic carbonate precipitation.

References

- [1] A. Maiti, J.K. Basu, S. De, Experimental and kinetic modelling of As(V) and As(III) adsorption on treated laterite using synthetic and contaminated groundwater: effects of phosphate, silicate and carbonate ions, *Chem. Eng. J.* 191 (2012) 1–12.
- [2] M. Ciopec, A. Negrea, L. Lupa, C. Davidescu, P. Negrea, P. Sfârloagă, Performance evaluation of the Fe-ir-120(na)-dehpa impregnated resin in the removal process of As(V) from aqueous solution, *J. Mater. Sci. Eng. 1* (2011) 421–432.
- [3] D. Borah, S. Satokawa, S. Kato, T. Kojima, Sorption of As(V) from aqueous solution using acid modified carbon black, *J. Hazard. Mater.* 162 (2009) 1269–1277.
- [4] Yoann Glocheux, Martín Méndez Pasarín, Ahmad B. Albadarin, Stephen J. Allen, G.M. Walker, Removal of arsenic from groundwater by adsorption onto an acidified laterite by-product, *Chem. Eng. J.* 228 (2013) 565–574.
- [5] M. Walker, R.L. Seiler, M. Meinert, Effectiveness of household reverse-osmosis systems in a Western U.S. region with high arsenic in groundwater, *Sci. Total Environ.* 389 (2008) 245–252.
- [6] T. Agusa, K. Takagi, R. Kubota, Y. Anan, H. Iwata, S. Tanabe, Specific accumulation of arsenic compounds in green turtles (*Chelonia mydas*) and hawksbill turtles (*Eretmochelys imbricata*) from Ishigaki Island, Japan, *Environ. Pollut.* 153 (2008) 127–136.
- [7] W. Shao, X. Li, Q. Cao, F. Luo, J. Li, Y. Du, Adsorption of arsenate and arsenite anions from aqueous medium by using metal(III)-loaded amberlite resins, *Hydrometallurgy* 91 (2008) 138–143.
- [8] I. Cano-Aguilera, N. Haque, G.M. Morrison, A.F. Aguilera-Alvarado, M. Gutiérrez, J.L. Gardea-Torresdey, G. de la Rosa, Use of hydride generation-atomic absorption spectrometry to determine the effects of hard ions, iron salts and humic substances on arsenic sorption to sorghum biomass, *Microchem. J.* 81 (2005) 57–60.
- [9] A. Goswami, P.K. Raul, M.K. Purkait, Arsenic adsorption using copper (II) oxide nanoparticles, *Chem. Eng. Res. Des.* 90 (2012) 1387–1396.
- [10] F. Partey, D. Norman, S. Ndur, R. Nartey, Arsenic sorption onto laterite iron concretions: temperature effect, *J. Colloid Interface Sci.* 321 (2008) 493–500.
- [11] Z. Li, R. Beachner, Z. McManama, H. Hanlie, Sorption of arsenic by surfactant-modified zeolite and kaolinite, *Microporous Mesoporous Mater.* 105 (2007) 291–297.
- [12] M.A. Subhan, S.A. Monim, M.B.R. Bhuiyan, A.N. Chowdhury, M. Islam, M.A. Hoque, Synthesis, characterization of a multi-component metal oxide (Al_{0.88}Fe_{0.67}Zn_{0.28}O₃) and elimination of As(III) from aqueous solution, *Open. J. Inorg. Chem.* 1 (2011) 9–15.
- [13] T.H. Boyer, A. Persaud, P. Banerjee, P. Palomino, Comparison of low-cost and engineered materials for phosphorus removal from organic-rich surface water, *Water Res.* 45 (2011) 4803–4814.
- [14] R. Li, Q. Li, S. Gao, J.K. Shang, Exceptional arsenic adsorption performance of hydrous cerium oxide nanoparticles: Part A. Adsorption capacity and mechanism, *Chem. Eng. J.* 185–186 (2012) 127–135.

- [15] G. Zhang, Z. Ren, X. Zhang, J. Chen, Nanostructured iron(III)–copper(II) binary oxide: a novel adsorbent for enhanced arsenic removal from aqueous solutions, *Water Res.* 47 (2013) 4022–4031.
- [16] A.B. Albadarin, C. Mangwandi, A.A.H. Al-Muhtaseb, G.M. Walker, S.J. Allen, M.N.M. Ahmad, Kinetic and thermodynamics of chromium ions adsorption onto low-cost dolomite adsorbent, *Chem. Eng. J.* 179 (2012) 193–202.
- [17] C. Mangwandi, A.B. Albadarin, Y. Glocheux, G.M. Walker, Removal of orthophosphate from aqueous solution by adsorption onto dolomite, *J. Environ. Chem. Eng.* 2 (2014) 1123–1130.
- [18] G.M. Walker, L. Hansen, J.A. Hanna, S.J. Allen, Kinetics of a reactive dye adsorption onto dolomitic sorbents, *Water Res.* 37 (2003) 2081–2089.
- [19] Y. Salameh, N. Al-Lagtah, M.N.M. Ahmad, S.J. Allen, G.M. Walker, Kinetic and thermodynamic investigations on arsenic adsorption onto dolomitic sorbents, *Chem. Eng. J.* 160 (2010) 440–446.
- [20] G.M. Walker, G. Connor, S.J. Allen, Kinetics of iron(II) removal from aqueous solution using activated dolomite, *Open Chem. Eng. J.* 1 (2007) 23–29.
- [21] T.-Y. Mun, J.-S. Kim, Air gasification of dried sewage sludge in a two-stage gasifier. Part 2: calcined dolomite as a bed material and effect of moisture content of dried sewage sludge for the hydrogen production and tar removal, *Int. J. Hydrogen Energy* 38 (2013) 5235–5242.
- [22] K. Sasaki, M. Yoshida, B. Ahmmad, N. Fukumoto, T. Hirajima, Sorption of fluoride on partially calcined dolomite, *Colloids Surf. A* 435 (2013) 56–62.
- [23] P. Staszczuk, E. Stefaniak, B. Biliński, E. Szymański, R. Dobrowolski, S.A.A. Jayaweera, Investigations on the adsorption properties and porosity of natural and thermally treated dolomite samples, *Powder Technol.* 92 (1997) 253–257.
- [24] A. Luque, B. Leiss, P. Álvarez-Llore, G. Cultrone, S. Siegesmund, E. Sebastian, C. Cardell, Potential thermal expansion of calcitic and dolomitic marbles from Andalusia (Spain), *J. Appl. Cryst.* 44 (2011) 1227–1237.
- [25] F. Boucif, K. Marouf-Khelifa, I. Batonneau-Gener, J. Schott, A. Khelifa, Preparation, characterisation of thermally treated Algerian dolomite powders and application to azo-dye adsorption, *Powder Technol.* 201 (2010) 277–282.
- [26] K.A.G. Gusmão, L.V.A. Gurgel, T.M.S. Melo, L.F. Gil, Adsorption studies of methylene blue and gentian violet on sugarcane bagasse modified with EDTA dianhydride (EDTAD) in aqueous solutions: kinetic and equilibrium aspects, *J. Environ. Manage.* 118 (2013) 135–143.
- [27] E. Stefaniak, B. Biliński, R. Dobrowolski, P. Staszczuk, J. Wójcik, The influence of preparation conditions on adsorption properties and porosity of dolomite-based sorbents, *Colloids Surf. A* 208 (2002) 337–345.
- [28] R. Otsuka, Recent studies in the decomposition of the dolomite group by thermal analysis, *Thermochim. Acta* 100 (1986) 69–80.
- [29] S. Karaca, A. Gürses, M. Ejder, M. Açıkıldız, Adsorptive removal of phosphate from aqueous solutions using raw and calcinated dolomite, *J. Hazard. Mater.* 128 (2006) 273–279.
- [30] G.M. Walker, G. Connor, S.J. Allen, Copper (II) removal onto dolomitic sorbents, *Chem. Eng. Res. Des.* 82 (2004) 961–966.
- [31] Yuttasak Chammui, Ponlayuth Sooksamiti, Wimol Naksata, Sakdiphon Thiansem, O.-A. Arqueropanyo, Removal of arsenic from aqueous solution by adsorption on Leonardite, *Chem. Eng. J.* 240 (2014) 202–210.
- [32] I. Andjelković, D.D. Manojlović, D. Djordjević, B. Dojčinović, G. Roglić, L. Ignjatović, Arsenic removal from aqueous solutions by sorption onto zirconium- and titanium-modified sorbents, *J. Serb. Chem. Soc.* 76 (2011) 1427–1436.
- [33] A. Duffy, G.M. Walker, S.J. Allen, Investigations on the adsorption of acidic gases using activated dolomite, *Chem. Eng. J.* 117 (2006) 239–244.
- [34] A. Dąbrowski, Adsorption – from theory to practice, *Adv. Colloid Interface Sci.* 93 (2001) 135–224.
- [35] J.D.S. Macedo, N.B. da Costa Júnior, L.E. Almeida, E.F.D.S. Vieira, A.R. Cestari, I.D.F. Gimenez, N.L. Villarreal Carreño, L.S. Barreto, Kinetic and calorimetric study of the adsorption of dyes on mesoporous activated carbon prepared from coconut coir dust, *J. Colloid Interface Sci.* 298 (2006) 515–522.
- [36] S. Lagergren, Zur theorie der sogenannten adsorption gelöster stoffe *KungligaSvenska Vetenskapsakademiens, Handlingar* 24 (1898) 1–39.
- [37] Y.S. Ho, G. McKay, Pseudo-second order model for sorption process, *Process Biochem.* 34 (1999) 451–465.
- [38] L. Khezami, R. Capart, Removal of chromium(VI) from aqueous solution by activated carbons: kinetic and equilibrium studies, *J. Hazard. Mater.* 123 (2005) 223–231.
- [39] B.H. Hameed, M.I. El-Khaiary, Malachite green adsorption by rattan sawdust: isotherm, kinetic and mechanism modelling, *J. Hazard. Mater.* 159 (2008) 574–579.
- [40] Y.S. Al-Degs, M.I. El-Barghouthi, M.A. Khraisheh, M.N.M. Ahmad, S.J. Allen, Effect of surface area, micropores, secondary micropores, and mesopores volumes of activated carbons on reactive dyes adsorption from solution, *Sep. Sci. Technol.* 39 (2010) 97–111.
- [41] I. Langmuir, The constitution and fundamental properties of solids and liquids, *J. Am. Chem. Soc.* 38 (1916) 2221–2295.
- [42] H.M.F. Freundlich, Over the adsorption in solution, *J. Phys. Chem.* 57 (1906) 385–471.
- [43] O. Redlich, D.L. Peterson, A useful adsorption isotherm, *J. Phys. Chem.* 63 (1959) 1024–1026.
- [44] D. Mohan, C.U. Pittman Jr., Arsenic removal from water/wastewater using adsorbents—a critical review, *J. Hazard. Mater.* 142 (2007) 1–53.